Supplementary Information for

Optical Fiber-Driven Low Energy Electron Gun for Ultrafast Streak Diffraction

Chiwon Lee, Günther Horst Kassier, and RJ Dwayne Miller *
*To whom correspondence should be addressed. email: dwayne.miller@mpsd.mpg.de

This PDF file includes:

1) Estimation of the temporal broadening of the triggering pulse
2) Description of the ASTRA code simulation
3) Synchronization scheme of the streak camera triggering pulse with respect to the electron bunch entrance timing

Estimation of the temporal stretching of the triggering pulse

We discuss four kinds of dispersion that can affect stretching of the laser pulse width during propagation inside a fiber [1].

1) Modal dispersion, σ_m

Each mode propagating inside the large core multimode fiber has different group velocities. The rms pulse width owing to the modal dispersion inside the fiber, σ_m, is a function of the fibre length, L , and numerical aperture of the fiber (*NA*), and refractive index of the core (n_1).

$$\sigma_m = \frac{L \cdot NA^2}{4 \cdot c_0 \cdot n_1}$$

The *NA* of the fiber used in the present experiment is 0.228127, L = 1 m, n_1 =1.46, thereby yielding σ_t = 31.19 ps. This value is the theoretical maximum of the modal dispersion-induced pulse stretching, assuming that the incoming free space beam is coupled to the fiber with the same *NA* as the nominal *NA* value of the fibre.

The effective numerical aperture due to the actual coupling condition, $NA_{effective}$, is different from the nominal *NA* of the fiber, and has to be taken into account to estimate the actual value of σ_m during the experiment [2], and can be written as

$$NA_{effective} = n \cdot \sin\theta$$

where, n is the refractive index of the free space medium (=1 for air), and θ is the half-angle of the cone of the converging light from the lens into the fiber.

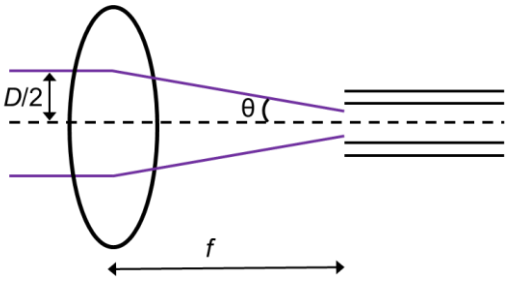

Figure S1. Illustration of free space-to-fiber coupling

In the experiment, we used a focusing lens with a focal length of 40 mm for the purpose of free space beam-to-fiber coupling, and the rms beam size (*D*/2) of the free space beam was 525 μm. From these values, $NA_{effective}$ is calculated as 0.01312, approximately a factor of 17 smaller than the nominal *NA* of the fiber. The actual σ_m is then estimated as 98 fs.

2) Material dispersion, σ_{mat}

When the free space laser pulse composed of a spectrum of different wavelengths is coupled to the fiber, each wavelength component travels with a different group velocity inside the fiber core. As a result, the initial temporal pulse width in the free space spreads after propagating a distance. The pulse stretching caused by this material dispersion, σ_{mat}, is described as follows:

$$\sigma_{mat} = D_{mat} \cdot \sigma_{\lambda} \cdot L$$

where D_{mat} and σ_{λ} are the material dispersion coefficient and the spectral width of the free space laser, respectively. D_{mat} is 5174 ps/km-nm, as specified by the fiber supplier. σ_{λ} is measured as 1.09 nm (RMS) at the central wavelength of 257 nm. Thus, σ_{mat} = 5.64 ps.

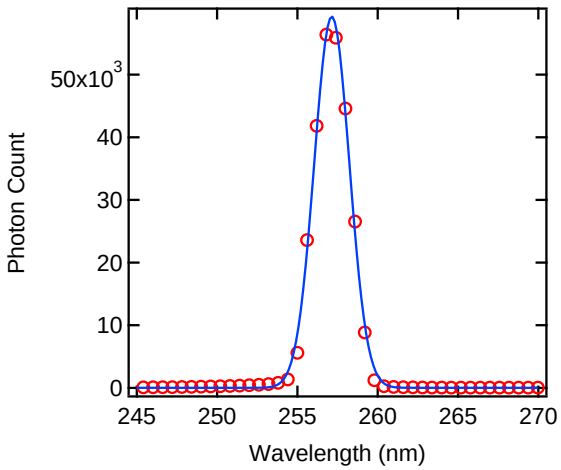

Figure S2. Wavelength spectrum of the trigger laser pulse

3) Waveguide dispersion, σ_w

Waveguide dispersion arises owing to the different phase velocities in the core and cladding when the pulse travels inside the fiber. It is significant in single mode fibers, but not in large core multimode fibers in which the field distribution ratio between the core and the cladding is large. The pulse stretching owing to the waveguide dispersion is described as

$$\sigma_w = D_w \cdot L \cdot \sigma_{\lambda}$$

where, D_w is the waveguide dispersion coefficient, expressed by the following relation:

$$D_w(ps \cdot nm^{-1} \cdot km^{-1}) \approx -\frac{83.76 \cdot \lambda(\mu m)}{[a(\mu m)^2 n_2]}$$

Here a and n_2 are the fiber core diameter and refractive index of the cladding, respectively. Given the 100 μm core size of the present fiber, we neglect the effect of the waveguide dispersion in considering the pulse stretching.

4) Nonlinear dispersion, σ_n

Due to the relatively low power of the incoming light and the large size of the core, we neglect any nonlinear dispersion effect in the pulse stretching.

Finally, based on the above discussion, modal and material dispersion effects contribute to the overall temporal stretching of the laser pulse, leading us to conclude that the estimated rms temporal width of the laser pulse, σ_{total}, after propagation of 1 m of the fibre is 5.81 ps

($\sum \sigma_{total}^2 = \sum \sigma_m^2 + \sum \sigma_{mat}^2 + \sum \sigma_{initial\_RMS\_pulse\_width}^2$). With an assumption of Gaussian temporal profile (Fig. 4(d) in the main text), this value is equal to the FWHM width of 13.69 ps.

Description of the ASTRA code simulation

ASTRA is a space charge tracking solver based a mean-field approach.

1) The longitudinal electric field component on the longitudinal position on the radial-symmetry axis is calculated in the case of maximum focusing condition corresponding to V_{lens} of 1.22 kV at $V_{cathode}$ of 1.6 kV with a commercial software package (CST particle studio), and is exported to the ASTRA particle tracking code for defining the actual electrostatic fields nearby the electron beam propagation. The radial and magnetic field components are deduced from the derivative of the longitudinal field with respect to the longitudinal position, automatically from ASTRA.

2) To simulate photoelectron generation on our optical fiber-based cathode in ASTRA, we set 1000 particles generated from a circular spot with 100 um rms diameter. The actual number of electrons per bunch is reflected by adjusting the bunch charge parameter. In the emission spot, the transverse and longitudinal spatial distributions of the electrons are assumed to have a Gaussian profile. The effective work function of the gold layer is assumed to 4.3 eV and the photon energy is set to 4.824 eV corresponding to the 257 nm wavelength of the triggering laser pulse. The initial momentum distribution of the electrons in the transverse and longitudinal axis is assumed to have a Fermi-Direc distribution at 300 K. Given those assumptions, ASTRA simulator calculates the rms electron kinetic energy spread, σ_{Ekin}, by the following formula [3]:

$$\sigma_{Ekin} = \frac{1}{3\sqrt{2}}(E_{phot} - \phi_{eff})$$

The calculated rms energy spread is equal to 0.12 eV (= 0.28 eV FWHM), which is in good agreement with the reported value of a photocathode made of the thin gold film on a sapphire substrate [4]. This calculated value is taken into account during the entire particle tracking simulation. We also note that the measured rms spectral width (0.02 eV equal to 1.09 nm, as shown in Figure S(2)) of the photo injection trigger beam is only approximately 17 % of the energy spread caused by the photoemission process. Therefore, we expect the effect of the broadened spectra of the trigger beam is negligible to the simulated electron bunch length.

3) In ASTRA, the space charge field is calculated on a cylindrical coordinate based volume. We sectioned this space charge field volume into 5 rings in the radial direction and 8 slices in the longitudinal direction, indicating that on average 25 particles are contained in each sectioned grid in the simulation.

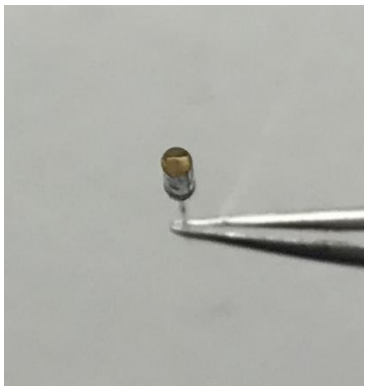

Figure S3. Gold layer coated fiber ferrule and fiber

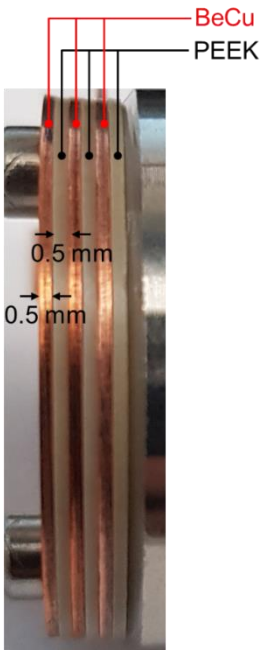

Figure S4. Photograph of the Einzel lens system. The material used for the conducting and insulating plate is BeCu and PEEK, respectively.

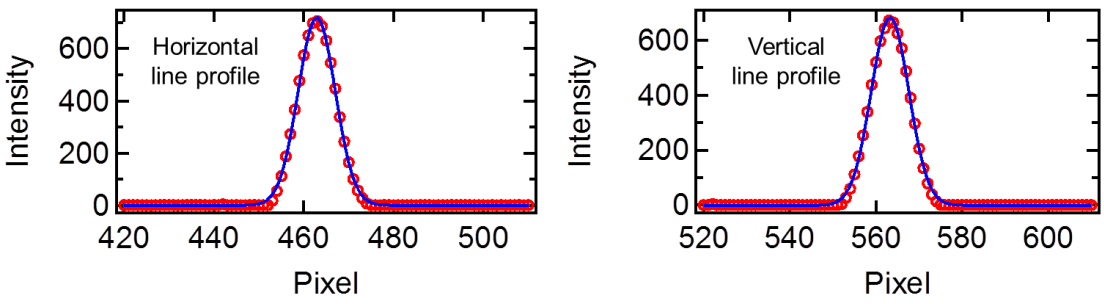

Figure S5. Horizontal and vertical line profile of the beam spot imaged on the screen at V_{lens} equal to 1.2 kV. The blue curve indicates the Gaussian fit and the red circle is the measured data.

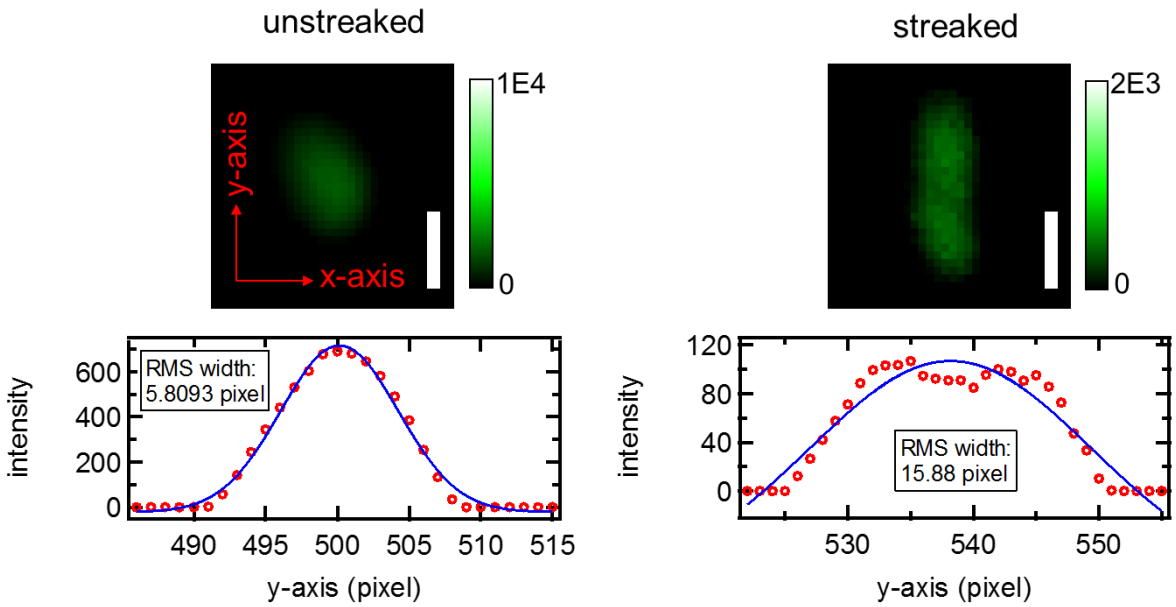

Figure S6. Line profile of the beam spot in y-axis direction after binning pixels in x-direction.

Synchronization scheme of the streak camera triggering pulse with respect to the electron bunch entrance timing

As illustrated in Figure 4(a) of the main text, we vary the travel distance of the streak camera triggering pulse by moving the mirror placed on the delay line stage. The travel distance of the photoinjection pulse is fixed. In this way, we are able to control the arrival time of the streak camera triggering pulse with respect to that of the photoinjection pulse.

In order to find the maximum streak velocity region (typically in the first zero-crossing where the linear field ramp-up or –down appears), we image the electron beam spot on the screen and compare the streaked beam spot positions to that of the unstreaked one, as shown in Figure S7.

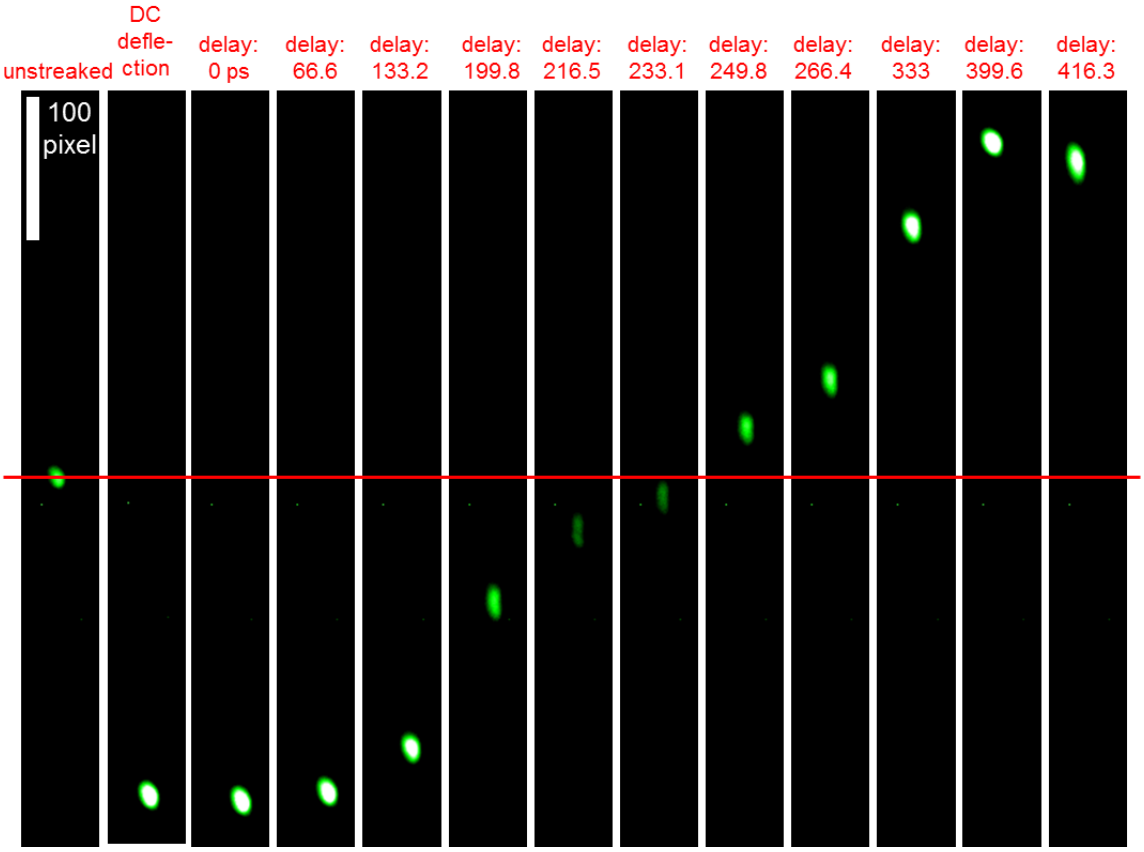

Figure S7. Change of the electron beam spot position as a function of relative delay between the streak camera triggering beam and the electron bunch entrance timing.

<Reference>

1. B.E.A. Saleh and M.C. Teich, *Fundamentals of Photonics* (John Wiley & Sons, Inc., 1991), p272-p309

2. E. A. J. Marcatili, *Modal dispersion in Optical Fibers With Arbitrary Numerical Aperture and Profile Dispersion*, The Bell System Technical Journal, 56(1), 49 (1977)

3. http://www.desy.de/~mpyflo/Astra_manual/Astra-Manual_V3.2.pdf, p104

4. A. Janzen et al., Rev. Sci. Instrum., 78, 013906 (2007)